A. Materka, M. Strzelecki, R. Lerski, L. Schad: *Scanner Resolution and Noise Influence on Texture Parameters of Magnetic Resonance Phantom Images*, International Conference "Computers in Medicine", 23-25 September 1999, Łódź, Poland, 101-107.

SCANNER RESOLUTION AND NOISE INFLUENCE ON TEXTURE PARAMETERS OF MAGNETIC RESONANCE PHANTOM IMAGES

Andrzej Materka, Michał Strzelecki, Institute of Electronics, Technical University of Łódź, Stefanowskiego 18, 90-924 Łódź, Poland
Richard Lerski, Medical Physics Department, Ninewells Hospital and Medical School, Dundee DD1 9SY, United Kingdom
Lothar Schad, Deutsches Krebsforschungszentrum Abt. Radiologie, Im Neuenheimer Feld 280, D-69120 Heidelberg, Germany

Abstract

Texture parameter analysis of test object (phantom) magnetic resonance images (MRI) is described in this paper. The test objects are made of different-porosity reticulated foam embedded in agarose gel. Optical images are analyzed in this paper, split into classes differing by the foam pore size. First- and second-order statistical features are computed. Their usefulness to texture class discrimination is evaluated using the ratio *F* of between-classes variance to within-classes variance. The effects of image normalization on *F*, and mutual dependence between features are investigated.

1. Introduction

The objective of this paper is to present results of a preliminary study on texture analysis of MR phantom images. Prior studies have been carried out [3] to investigate whether texture measurements are transportable between magnetic resonance centers and to make firm conclusions as to the machine settings and sequence selection required. Development of quantitative methods of texture analysis of magnetic resonance images is now the subject of COST B11 European Community project scheduled for the years 1998-2002 [2]. The aim of this project is to develop methods for reliable discrimination of different kinds of tissue in MR images, independent of scanner type, parameters or settings.

2. Test object images

The use of texture analysis in magnetic resonance imaging requires the availability of texture test objects for use in standardization of *in vivo* measurements. The reticulated foam materials were used in this study. Optical images of these objects were digitally recorded. They contain scans of cross-section of two different-porosity foams (Fig. 1). From each optical image, 42 non-overlapping samples of size 23x23 pixels were taken, resulting in 2 texture classes, each of 42 samples.

3. Results and discussion

A number of subroutines in Matlab and a specialized MS Windows application program MaZda [2] were written to compute a variety of texture features (parameters). The programs were applied to the recorded MR and optical images to compute texture features and thus characterize texture properties.

a) 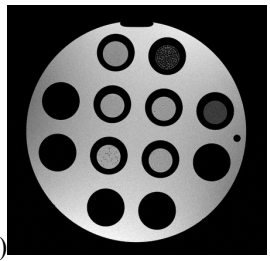 b) 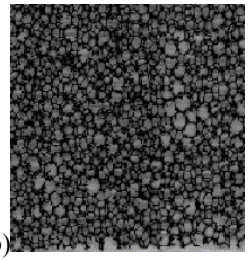 c) 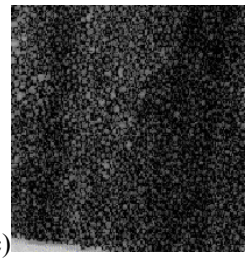

Fig. 1 a) MR slice image of tubular phantoms; b), c) optical images of reticulated foam materials: b) Foam1 – large pore size, b) Foam2 – medium pore size.

To investigate any feature ability to discriminate between different pore-size textures, the following F coefficient was used:

$$F = \frac{D}{V} \tag{1}$$

that represents the ratio of between-classes feature variance D to within-classes feature variance V [4]. For each sample (region of interest – ROI) of an optical image, the following 254 features were calculated:

- H: 9 histogram-based (mean, variance, skewness, kurtosis and five histogram percentiles for 1%, 10%, 50%, 90%, and 99%: #1 – #9),
- GR: 5 gradient-based features (absolute gradient mean, variance, skewness, kurtosis, and percentage of non-zero gradients: #10 – #14),
- RL: 20 run-length matrix-based features (short run emphasis inverse moment, long run emphasis moment, gray level nonuniformity, run length nonuniformity and fraction of image in runs, separately for horizontal, vertical, 45° and 135° directions: #15 – #34),
- CO: 220 co-occurrence matrix based features (11 features defined in (Haralick 1973) calculated for matrices constructed for five distances between

image pixels (d=1, 2, 3, 4 and 5), and for the four directions as in the case of RL features: #35 – #254.

Except for the histogram-based features, each ROI image was quantized to 64 gray levels (6-bit word-length) prior to computation of the texture parameters.

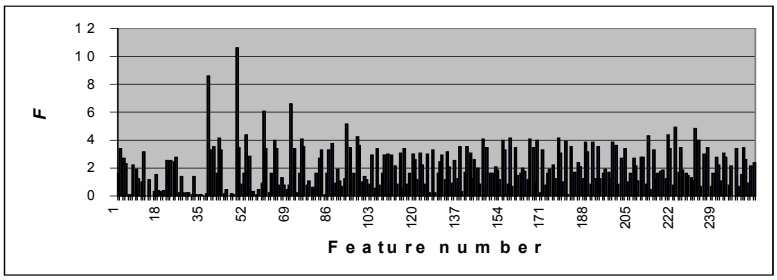

Fig. 2 *F* coefficient for H, GR, RL and CO features (no ROI normalization).

As presented in Fig. 2 for raw images, only 4 features from the whole set (#37, #48, #59, and #70) represent relatively high value of *F* coefficient (e.g. $F \geq 6.0$). They are Correlation parameters calculated for the co-occurrence matrix determined at $d = 1$, for the four main directions. Other features possess lower *F* values, which means that they are not much useful to make distinction between the two classes of the foam texture, cf. Table 1.

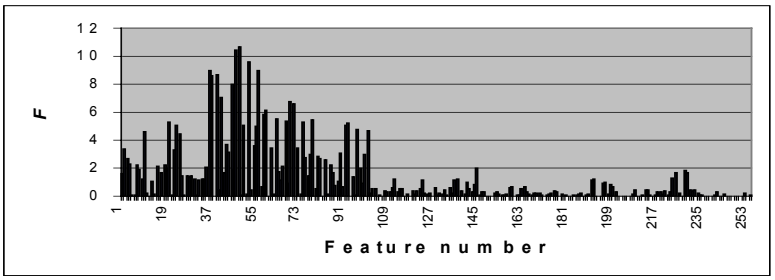

Fig. 3 *F* coefficient for H, GR, RL and CO features ('±3 sigma' normalization).

To investigate whether image normalization affects feature ability to allow discrimination between the image classes, two normalization schemes were considered. For both schemes, the image histogram was first computed within each ROI. Then, the image mean μ and standard deviation σ were found. For the '±3 sigma' scheme, the image intensity levels were limited to the range from $f_{min}=\mu-3\sigma$ to $f_{max}=\mu+3\sigma$. The intensity range (f_{max}–f_{min}) was then quantized using 6-bit word-length prior to computation of GR, RL and CO parameters. For the '1%–99%' scheme in turn, the values of f_{min} and f_{max} were found as corresponding to, respectively, 1% and 99% of cumulative image histogram within ROI.

The *F* coefficient distribution among the different texture features, obtained for the '±3 sigma' normalization scheme is illustrated in Fig. 3. Indeed, for this scheme, the number of features that have high *F* ($F \geq 6.0$) increased significantly

to 12. An intermediate number of 9 such features was obtained for '1%–99%' scheme. Numerical results of this experiment are presented in Table 1.

As can be observed in Table 1, all the features with relatively high value of *F* are derived from CO matrix. What is more, only one of them (Sum Variance, #96) is computed for distance between image pixels larger then one. This means that larger distances do not produce useful parameters for discrimination of the discussed textures. This can be explained by analysis of Fig. 4. It shows cross-sections of correlation function calculated for sample ROI for Foam1 and Foam2 images. This function rapidly decreases when distance between pixels is larger then one. This suggest that there is no important information concerning analyzed images contained in CO matrices constructed for distances between image pixels larger then one.

Table 1
F coefficient for different normalization schemes (shaded areas: $F>6$).

No.	Feature definition	Feature number	*F*, no normalization	*F* '±3 sigma'	*F* '1%–99%'
1	(1,0) Contrast	36	0.2	9.0	2.4
2	(1,0) Correlation	37	8.7	8.6	8.8
3	(1,0) Inv. Differential Moment	39	3.5	8.7	5.5
4	(1,0) Sum Variance	41	4.1	7.1	7.0
5	(1,0) Differential Entropy	45	0.0	8.0	3.6
6	(0,1) Contrast	47	0.1	10.4	2.9
7	(0,1) Correlation	48	10.6	10.7	10.9
8	(0,1) Sum Variance	52	4.4	9.6	7.5
9	(0,1) Differential Entropy	56	0.1	9.0	3.4
10	(1,1) Correlation	59	6.1	6.2	6.1
11	(1,1) Sum Variance	63	4.0	5.6	6.3
12	(1,-1) Contrast	69	0.8	6.7	0.8
13	(1,-1) Correlation	70	6.6	6.6	6.7
14	(1,-1) Sum Variance	74	4.1	5.3	6.3
15	(0,2) Sum Variance	96	4.2	4.7	7.3

It is evident from Figs. 2 and 3 that the number of useful features depends significantly on image normalization. To explain this effect, one should refer to image properties as seen in Fig. 1. Namely, the images investigated, especially 'Foam2', show some nonuniformity of their local mean and variance. It can be found that relative standard deviation σ_μ of image mean μ, computed over 48 ROIs, is equal to $\sigma_\mu/\mu=12.2\%$ for 'Foam1' and as much as $\sigma_\mu/\mu=24.2\%$ for Foam2. Similarly, the corresponding ratios related to image variance are equal to 15.8% for 'Foam1' and 29.1% for 'Foam2'. (At the same time, *F* coefficient for image mean μ is equal to 1.6 and that for image variance σ^2 equals to 3.4.) One can then expect that if there exist texture features, which possess high correlation to μ and σ^2, and image is not normalized, then such features will demonstrate non-zero values of *F* even if they do not carry any information about texture properties other than included in μ and σ^2. At the same time, their *F* values will be rather moderate, as the *F* values for μ and σ^2 are. Such features will be redundant in the

considered application. Moreover, high correlation to μ and σ^2 may mask an existing ability of a feature to discriminate the texture classes.

To find out whether there are indeed features highly correlated to μ and σ^2 for the two textures in Fig. 1, the correlation coefficients for of each of the 254 features with both μ and σ^2 were calculated – without, and with '±3 sigma' image normalization. Calculation results are presented in Fig. 5. As can be observed, for the non-normalized images most features are highly correlated with image mean. Only the Correlation feature derived from CO matrices is relatively independent of it (Fig. 5a). After '±3 sigma' normalization, the correlation coefficient value significantly decreases in case of both textures (Fig. 5b). Similar observation can be made for image variance, which is highly correlated to image mean in the case of discussed images (correlation coefficient equal to 0.89 and 0.97, respectively for Foam1 and Foam2).

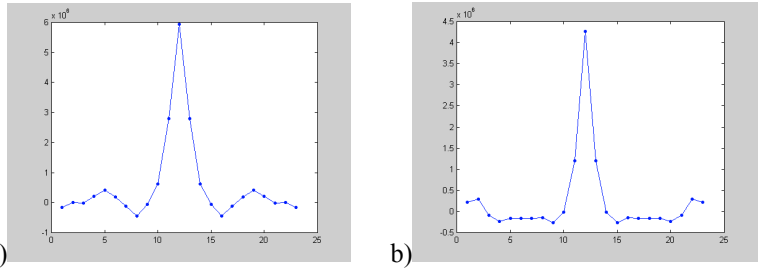

a) b)

Fig. 4 Cross-section of correlation function for a sample ROI: a) Foam1, b) Foam2.

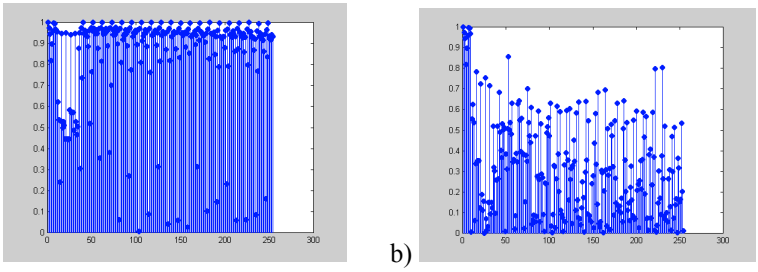

a) b)

Fig. 5 Feature correlation to image mean: a) no normalization, b) '±3 sigma' normalization, obtained for Foam2 image.

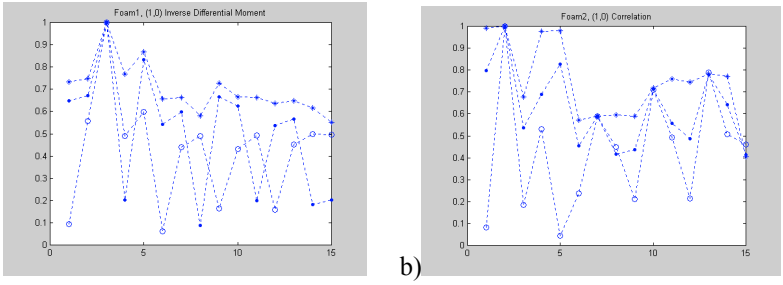

a) b)

Fig. 6 Absolute value of correlation coefficient between parameters from Table 1 and a) (1,0) Inverse Differential Moment, b) (1,0) Correlation, ° no normalization, + "±3 sigma", • "1%-99%".

More detailed analysis shows that standard deviation of the mean of Foam1 equals to 7.8, 0.2, and 4.5, respectively for 'no normalization', '±3 sigma', and '1%-99%' schemes. The corresponding figures for 'Foam2' are equal to 11.3, 0.2, and 3.5. Thus '±3 sigma' scheme provides the best stabilization of the image mean value within the (f_{max}–f_{min}) window. This results in the highest number of the discriminative features (Fig. 3), thanks to elimination of the effect of their correlation to mean and variance [μ=0 and σ^2 is constant relative the (f_{max}–f_{min}) range for '±3 sigma' scheme]. Table 1 indicates that CO Correlation does not indeed depend on image normalization.

On the other hand, the '±3 sigma' normalization causes increase of correlation between texture parameters. This is shown in Fig. 6. As can be observed, correlation between sample parameters and other texture features is relatively high for '±3 sigma' normalization in the case of both textures. Similar results can be observed for other parameters from Table 1, except for Sum Variance, which can be explained based on this feature definition [1]. This means, that the number of texture parameters useful for texture discriminations is in fact limited due to relatively high correlation between them.

4. Conclusions

Initial evaluation of statistical parameter effectiveness to discriminate between two test-foam objects for MRI has been carried out. Surprisingly, only a few among more than 200 popular features turned out useful to distinguish the otherwise quite distinct (at least for humans) textures. This indicates the need for carrying on research work on better understanding of texture properties and for finding new feature definitions that would provide means for firm discrimination of different images of biological origin. The significance of image normalization prior to texture parameter computation has been demonstrated. For the future, the following investigations are planned:

- consideration of new texture features (e.g. wavelet-based),
- analysis of noise influence on classification accuracy for different features,
- further development of MaZda software used for feature calculation,
- development of feature selection methods for MR image texture,
- extension of the results to texture classification of biological tissue.

It is expected that the new computer-based texture analysis techniques will automate part of the medical diagnosis process, assuring its objectivity and repeatability.

Acknowledgement: This work is part of COST B11 European project. It was also supported by British-Polish Joint Research Programme.

References

[1] R. Haralick, K. Shanmugam and I. Dinstein, Textural Features for Image Classification, IEEE Trans. Systems Man Cybernetics, 1973, vol. 3, pp. 610-621.
[2] Internet 1999, http://phase.pki.uib.no/~costb11/
[3] R. Lerski, K. Straughan, L. Schad, D. Boyce, S. Bluml, I. Zuna, "MR Image Texture Analysis – An Approach to Tissue Characterization", Magnetic Resonance Imaging, 1993, vol. 11, pp. 873-887.
[4] J. Shürmann, Pattern Classification, John Wiley and Sons, New York, 1996.